Active Electronic Egg For Breeding of Endangered Birds

Francisco J. Quiles-Latorre, Andrés Gersnoviez, Manuel Ortiz-López, Francisco J. Jiménez-Álvarez, Francisco J. Montoro-García, María Brox

***Abstract*— This work presents a prototype of an artificial egg for use in breeding centres for endangered birds. These eggs replace the inert artificial eggs that are given to the birds while the natural egg is incubated in the laboratory. When the chick hatches, it is given to the parents to continue breeding. This first prototype of the active egg is designed for the bearded vulture (Gypaetus barbatus), simulating the sounds and movements of the chick inside, and with the same appearance, size and weight as a natural one. The movements and sounds of the active artificial egg are made at the request of its caregiver and under his supervision and control in real time via a wireless connection. The active artificial egg has battery-powered circuitry inside that allows it to maintain wireless communication between the caregiver and the egg, because the egg must not perform autonomous physical actions at any time. This prototype has been tested for three seasons on a foster male and a natural couple of birds with good results because the birds have not rejected the prototype and have shown exactly the same behaviour exhibited when incubating a natural egg. The electronic system has among other circuits a microcontroller, a small motor to produce vibrations that simulate the movement of the chick and an mp3 player for the reproduction of sounds previously recorded on a microSD card. A low power consumption system has been designed to increase the autonomy of the device.**

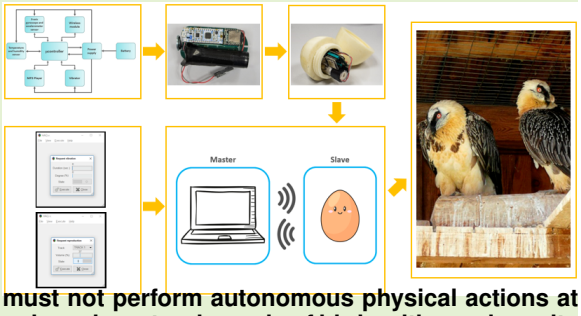

***Index Terms*— Electronic egg, low power system, microcontroller.**

I. Introduction

THE monitoring of wild animals to improve the conditions of these animals or to preserve endangered species [1] is a topic of great interest. The first way to get information from the animals was to use field observers, as in [2] where the behavior of apes is studied. Sometimes, the human access to areas where wild animals live to study their behavior is difficult due to problems such as the dense vegetation of their habitats. Also, the human presence can stress the animals by modifying their behavior and the information collected.

In order to solve these problems, in the early 2000's electronic devices began to be used to take data continuously and in real time. Mobile sensors placed on animals have been used. An example of this is GPS technology which is used for animal tracking as in [3] where a system to monitor and track the pink iguana in the Galapagos Islands is proposed; this work shows a device packed inside a transparent PVC enclosure which is attached to the body of the iguana and it is equipped with a low-power transceiver and a set of sensors (temperature, humidity, light sensor, GPS). As these species live in a habitat without power supply the device includes a small solar panel and a supercapacitor. GPS systems placed on animals are also proposed in [4] where a GPS datalogger is used to track the movements of African penguins and in [5] where GPS collars placed on elks capable of remote transmission of data to a command unit, are presented.

Nowadays, fixed sensors such as Wireless Sensor Networks (WSNs) are also widely used to retrieve information from animals. WSN technology allows the design of low-cost systems that facilitate this task of studying and monitoring of wildlife. [6]- [7] show that one of the current applications of WSNs is animal monitoring. [8] was one of the first proposed works using WSNs to monitor wildlife; this works presents a network of 32 nodes deployed on a small island for monitoring seabird nesting environment. In the same context [9]- [10] show other works proposed to monitor wildlife using WSNs. [9] presents a WSN system developed to monitor the animal's feeding and drinking behaviors. Other WSN to monitor environmental parameters (Temperature, Humidity and Light) that can alter the health of cows on a farm producing stress and disease, is proposed in [10].

These systems based on WSN have a power problem especially in outdoor environments. For this reason, in the development of this type of devices it is very important to achieve low power consumption. In [11]- [17] works with developments of monitoring devices for animals with low consumption are presented. [11] proposes a WSN deployed in Doñana National Park to collect information about the behavior of the animals in the park. A study of power consumption of the system and the analysis of the lifetime of batteries, is included. Other analysis of power consumption of the motes is performed in [12] where a network of five motes has been placed in a plantation of lettuces; this work presents a ZigBee WSN

Fig. 1. Bearded vultures in the Breeding Centre of Cazorla (Spain).

to detect the presence of snails in the field using collected environmental data by the WSN with the objective of avoiding the damage that snails cause to agricultural plantations. Other work that includes performances to achieve a reduction in power consumption and improve the lifetime of batteries is proposes in [13] where a WSN with low cost and low power sensor nodes is developed to monitor the health of cows. [14] presents the construction of a WSN for the monitoring of long-tailed ducks which is an endangered specie in the region of Artic; in order to reduce energy consumption, the authors propose that nodes be active and inactive, effectively increasing the system lifetime. In [15] the development of a WSN to divert animal intrusions in the crop field is presented; the power consumption of the nodes is reduced by including the Sleep modes wherever necessary and solar panels. Finally, with this same purpose, a very low consumption system for remote monitoring of bee colonies is purposed in [16]- [17].

Focusing on the particular application of this work, numerous studies of WSNs to monitor birds have been proposed [18]- [22]. In these works, sensors are used to detect the presence of birds by periodically collecting samples of bird songs. Other works monitoring bird behavior are based on the development of artificial eggs which collect information from sensors [23]- [24]. In the field of recovery of endangered birds and in particular, in the Bearded Vulture Breeding Centres (Gypaetus barbatus) under the European Endangered Species Programme (EPP), it is common to use plaster eggs to replace natural ones in the incubation [25]. In this way, the valuable natural eggs are incubated in the laboratory, especially at the final stage of the process, in order to be able to carefully control the embryonic development and attend to the delicate process of hatching (especially in pairs with double eggs laying or those that show alteration in their behavior during the hatching phase). Fig. 1 shows the image of a pair of bearded vultures in the Breeding Centre of Cazorla (Spain).

Furthermore, in the breeding system adopted by these Centres, it is essential that the chicks are fed and cared by parents. In this way, it is guaranteed that specimens will be obtained with an adequate imprint on their species so that they can reproduce normally when reaching sexual maturity, which is the final objective of the process of reintroduction of the species. But for that the bearded vultures do this natural breeding (of the chick born in the laboratory and out of parental care until then) it is of great importance that they keep the incubation of the artificial egg until the chick is delivered to them for adoption, because if they abandon it for any reason, they will lose their love for taking care of a chick and they will not be able to act as foster pair that season.

The artificial eggs that have been used for this purpose are built with solid plaster. Specifically, [23] presents the construction of an artificial egg for vultures that monitors the internal temperature of the egg, humidity, carbon dioxide levels, light intensity and egg rotation movements carried out by the birds in order to obtain a better knowledge of the actual incubation parameters. The system consists of three modules. A module for data collection, processing and storage, a module that receives the processed data and sends it wirelessly, and finally, a repository of data in the cloud, which can be consulted by researchers. The system in charge of data collection, processing and storage is implemented using a Raspberry Pi where a Microduino Core+ module, a Bluetooth module, a calendar clock (RTC) and a weather station module have been connected. The Raspberry Pi communicates with these modules via the serial bus. It is placed near the egg and receives the information collected by the egg's sensors. It also monitors weather conditions in the egg environment. All this information is stored and uploaded to the cloud when the system has Internet access.

Within this same purpose in [24] the incubation of bearded vultures by artificial eggs with data loggers in the Pyrenees is described. These eggs are equipped with three equidistant temperature and rotation sensors along with two humidity and two light sensors. The temperature sensors are located at 120 degrees to each other, so that there is always one in contact with the breast of the incubating bird and the other with the bowl, because the temperatures are different. Light sensors consist of photoelectric cells that when light is received indicate that the bird has risen to move or to receive the incubation relay in the pair. The stored data are then transferred to a computer for analysis of the information.

However, none of these conventional artificial eggs can provide the stimulation received by the parents in the incubation process when the chick moves within the egg or emits sounds close to hatching. In fact, there are specimens that have the ability to differentiate and reject plaster eggs and leave the incubation process if they do not receive such stimulus from the artificial egg. For this reason, it may be of great importance to develop artificial eggs that are indistinguishable from the natural ones and to have eggs that encourage the bearded vulture to maintain incubation.

In order to solve this problem, we have developed an active artificial egg. It is the first time in the world that an egg is built whose purpose is not only to collect data of incubation (temperature, humidity, frequency of turning, etc.) but also to produce to the bearded vulture a similar stimulus to that provided by a natural egg. In this sense, this work presents the development of an artificial egg prototype with a low power consumption that also makes measurements of temperature and humidity in the egg, and it is capable of emitting sounds analogous to those reproduced by the chick

and generated similar movements to that developed by the natural egg during the hatching process. So, the stimulation of the hatching process of the bearded vulture is more satisfactory and natural for the birds, and the possibility of rejection of the artificial egg decreases.

The exterior of the active artificial egg presented in this work is made of high resistance white plastic in order to guarantee that the bearded vulture, a large and very strong bird, cannot break it. It also allows remote interaction with the device by the Breeding Centre Technician, extracting information from sensors or executing commands (movements of vibration and sound), without the need to access to the nest in order not to disturb to the bird. The qualification of this technician is essential to send the necessary signals to the bird to produce the desired stimulus and to maintain the incubation instinct intact until the moment when the egg is removed and a chick is offered for adoption.

The structure of the article is as follows. Section II describes the general structure of the system as well as the materials used for the development of the artificial egg and size, range and consumption restrictions to be achieved by the device. The hardware design of the slave will also be discussed in this section. The communication protocol used for sending messages between the embedded system and the desktop application managed by the Breeding Centre Technician is also included. This section finishes with the development of the software for the master and slave system, respectively. Results of the consumption tests performed with the device will be included in the Section III. The work will end by showing the conclusions developed in Section IV.

II. Materials and Methods

This work shows the construction of an active prototype that is capable of handling the peripherals needed to emit sounds, vibrations, measures of the rotations, humidity and temperature measurements, receptions and emissions of radio frequency messages, all this reducing power consumption. In addition to consumption restrictions, an autonomy between 3 and 5 days must be achieved with a normal workload. When the egg performs any physical action, it must be controlled by the caregiver. It is not desired that the egg performs pre-programmed autonomous actions, given the lack of experience with these eggs.

The egg is made of a plastic called ABS (acrylonitrile butadiene styrene). The most important properties of this material are its resistance to impact and hardness. We have chosen white ABS because it is the color closest to that of a natural egg. Fig. 2(a), (b) and (c) show the initial prototype and Fig. 2(d), (e) and (f) show the final prototype.

Taking into account that dimensions of a bearded vulture egg are of the order of 90 mm in length, 68 mm in greatest diameter (34 mm of radius) and a weight of 230 grams, the construction of the prototype developed should have similar dimensions. The exact measurements of the prototype designed are 95 mm in outside height, 75 mm in greatest outside diameter and a weight of 250 grams; the interior cavity of the egg which includes the electronic device has 86 mm in internal height and 45 mm in greatest internal diameter. The two parts of the egg are joined by screw thread and it has been proven to be a safe mechanism and no bird has broken or opened it.

About the weight, it should be highlighted that a bearded vulture egg weighs around 180 grams. All the eggs of all the birds lose weight when the incubation progresses due to the evaporation of water from its interior as well as by the metabolism of the chick that also emits carbon dioxide through the pores of the eggshell. This weight loss is estimated to be about 15 % from start to finish of incubation and if, for some reason it is much less or much greater, the chances of successful hatching are dramatically reduced.

As can be deduced from these data, we have developed an egg whose weight and external measurements slightly exceed the largest of the normal eggs of the species. This is because all birds prefer slightly larger eggs than those of their species because the bird interprets that a larger and heavier egg is more probable to successfully develop into a stronger chick. They do not lay such large eggs because of an obvious problem of volume and because they cannot carry much weight for flight. For this reason, the artificial eggs that are used to replace the real ones in the Bearded Vulture Breeding Centres are heavier than the natural ones and can reach 250 grams. The aim is to make it easier for the bird to accept it and believe that it is a natural egg.

On the other hand, the embedded system software has also been developed to manage the internal peripherals of the microcontroller, as well as the external peripherals that are connected to it (communication module, sound player, vibrator and sensors) to handle the requests received from the desktop application.

The system follows a master/slave structure, as shown in Fig. 3. The master is a desktop application with a graphical interface, installed on a general-purpose computer. The developed graphical interface has been designed so that it is easy to use by non-experts and is compatible with Microsoft Windows operating systems. It communicates with the slave wirelessly, using an XBee module connected via USB [26]. The design guarantees communication at a distance of at least 30 meters so that the egg can be controlled by the Breading Centre Technician without being too close to the nest. A communication protocol has been designed for communication between master and slave.

The slave is an embedded system, capable of receiving commands and sending answers to the master, operating autonomously via a battery. When the slave receives a correct command from the master, it executes it and sends an answer to the master. The tasks that can be carried out are: to execute a vibration during a specified time, to reproduce a sound inside the egg, to send to the master information of temperature, humidity, state of the battery and state of the system.

A. Hardware Design of the Slave

Fig. 4 shows the block diagram of the designed system. It consists of the following blocks, which will be described later: Control, Power Supply, Vibrator, Wireless Communication, MP3 Player, Inertial Measurement Unit (IMU), and temperature and humidity sensor.

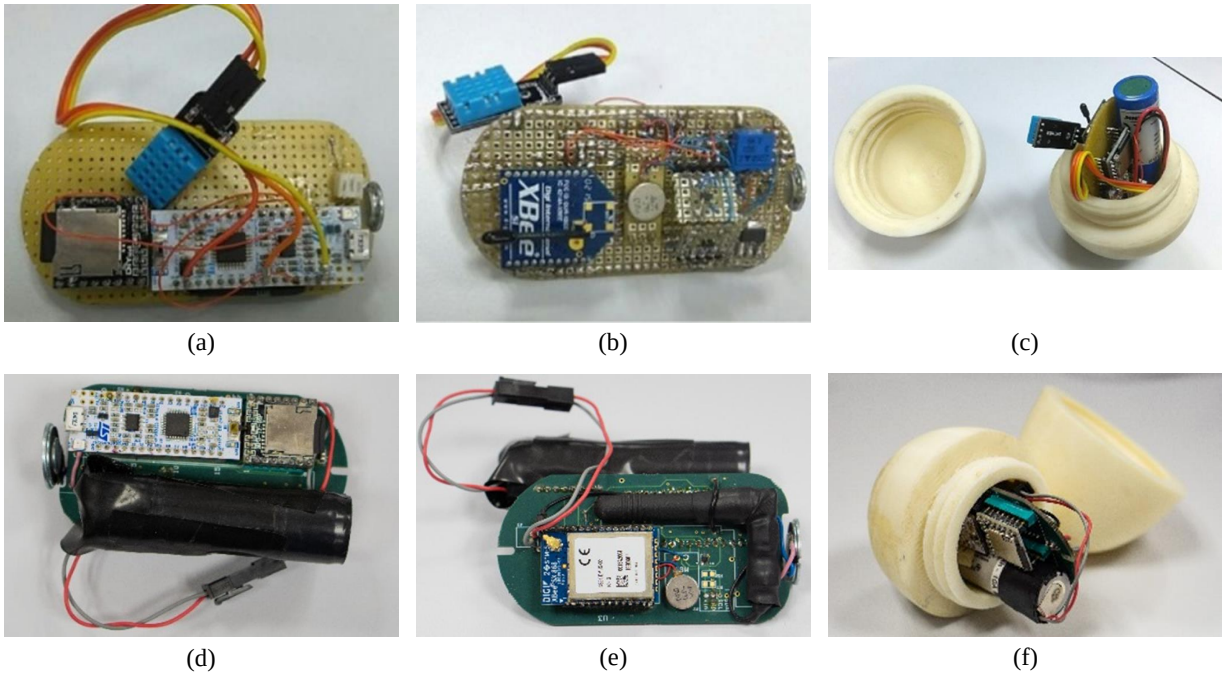

Fig. 2. (a, b and c) First predrilled prototype; (d ,e and f) Final prototype.

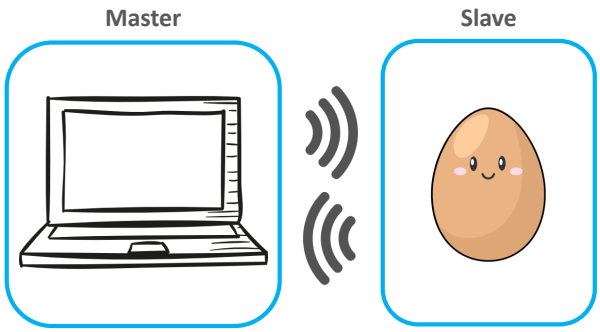

Fig. 3. General structure of the development system.

1) Control Block: It consists of a development board from the STElectronics company known as NUCLEO 303k8 [27], equipped with a STM32F303K8 [28] processor with a 32-bit Cortex M4 architecture and the circuits needed to program it via USB, which allows flexible and fast prototyping. This board has been selected, among other factors, for its small size and low power consumption, which is one of the main features of microprocessors with Cortex M ARM architecture. In addition, these processors can be programmed using a wide variety of high-level programming languages, and there are companies such as ARM limited [29], IAR Systems [30] and others that offer commercial compilers and development environments for ARM, in addition to other free tools such as those offered by ARM MBED [31]. Among the main technical features of this microcontroller are a 64 Kbyte flash memory, 12 Kbytes of SRAM, three low power consumption modes (standby, stop and deepsleep), two ADC with selectable resolution (12/10/8/6 bits), three 12-bit DAC channels, RTC calendar with alarm and periodic wakeup, three USARTs, up to 11 timers that can be configured as PWM, one bus I^2C and fast I/O ports.

Fig. 5 shows the connection diagram of the NUCLEO 303k8 board. For its operation it uses a 3.3 V power supply, generated by a Low DropOut regulator (LDO), whose characteristics will be analyzed in the section corresponding to the power supply block. The I^2C bus enables fast mode to speed up communication with the IMU and the temperature and humidity sensor. The STM32F303K8 includes configurable pull-up resistors that can be connected to the I^2C bus signals, but as these have a value higher than 4K7Ω, which is a recommended value to achieve a high transmission speed, it has been preferred to connect them externally. The description of the peripheral control signals and their functionality will be given in each subsection.

2) Wireless Communication Block: The Digi XBee SX 868 module is used for communication between master and slave [32]. This is an 868 MHz RF module that operates between 863 MHz and 870 MHz, making it deployable in several regions throughout the world including approved European countries. The module can run either a proprietary DigiMesh® or point-to-multipoint networking protocol. The Digi XBee SX 868 also leverages 868 MHz and surrounding frequencies for LBT + AFA (Listen Before Talk and Adaptive Frequency Agility). This significantly reduces interference by listening to the radio environment before any transmission starts, and by using a frequency of 868 MHz it allows a longer range than 2.4 Ghz modules, for the same transmission power. On the other hand, this module is widely used, does not require programming and has a high transmission power and low power consumption compared to series 1 and 2 modules. In addition, this module works as an independent co-processor and incorporates an UFL connector that allows an antenna to

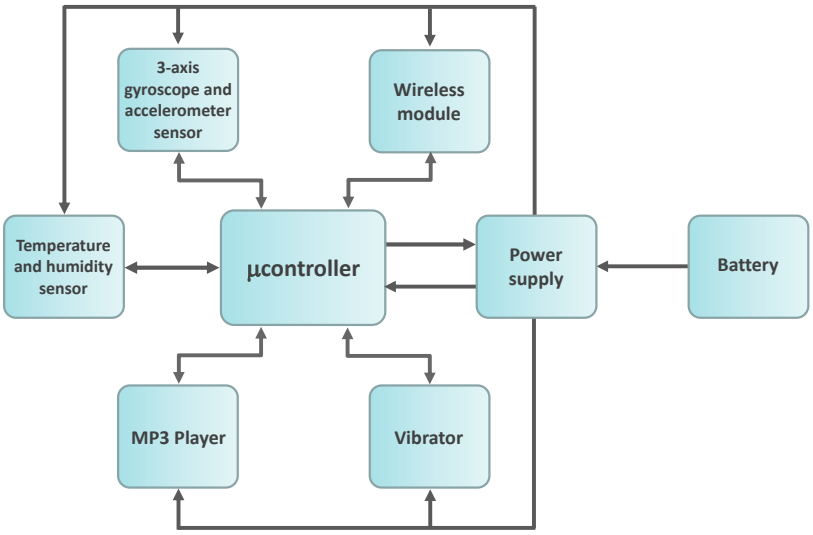

Fig. 4. Block diagram.

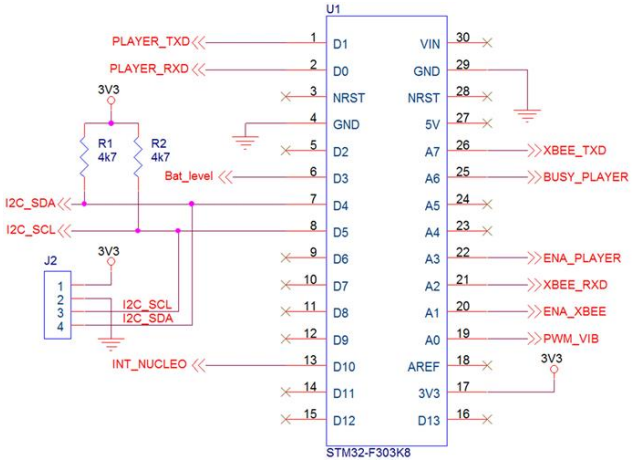

Fig. 5. Control block schematic.

be connected for longer range communication with the master system.

Although the system was initially designed for a single master to control several slaves, the tests carried out at the beginning of the project in the field led us to opt for a point-to-point connection. This avoids errors that the caregiver could make when selecting the slave egg. For this reason, Xbee module has been configured to work in transparent mode. When this mode is used, the XBee module pair works in such a way that the data received by the serial line are transmitted wirelessly. When an XBee receives data wirelessly, it sends it through the serial line just as it received it. This operating mode provides the same result as if both modules were connected with a pair of cables. Fig. 6(a) shows the wiring diagram of the Digi XBee SX 868 module.

The power supply of the XBee SX 868 module is 3.3 V (VCC_XBEE) which, as will be shown later, is generated from the battery voltage by an LDO regulator. The microcontroller communicates with the XBee module using only two signals: XBEE_TXD and XBEE_RXD. These two signals are used to implement UART-type communication, which allows the XBee module to be configured, receive commands from the host and send status information about the execution of these commands.

3) MP3 Player Block: For the reproduction of sounds the prototype also incorporates a DFPLAYER MP3 player [33], whose wiring diagram is shown in Fig. 6(b). This player was chosen because it has an adjustable sound level, uses a microSD memory card as a sound storage, so that the user can record the sounds to be played from a personal computer, and also includes an amplifier. This module can be controlled by the serial port which is connected to the UART1 of the microcontroller via the PLAYER_TXD and PLAYER_RXD signals. The PLAYER_TXD signal connects the transmission of the UART1 of the microcontroller to the reception of the DFPLAYER MP3, and sends the configuration and playback commands. The PLAYER_RXD signal connects the transmission of the DFPLAYER MP3 to the reception of the UART1 of the microcontroller, and through it the microcontroller receives information about the state of the MP3 player.

Busy pin of this module is activated at a low logic level while the DFPLAYER module is playing a sound with a delay of 19 milliseconds, and it is deactivated when the playback is over. This pin is connected via the BUSY_PLAYER signal to a port of the microcontroller, to check when a sound is playing and to cut the power to the module once it finishes the playback.

The DFPLAYER module operates in a power supply voltage range between 3.2 V and 5 V, and its current consumption values range is from 20 mA, without playing, to 200 mA, playing.

The power supply pin is connected to the positive terminal of the battery via a P-channel MOSFET. This reduces its power consumption by not applying battery voltage to it when it is not needed to play sounds.

A miniature loudspeaker with reference number KDMG1200805 [34] is also used for sound reproduction.

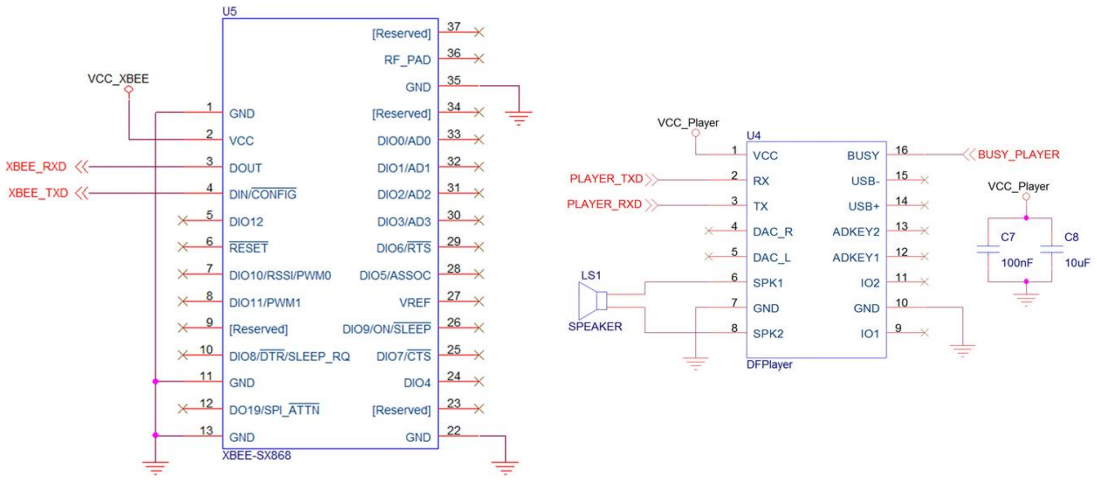

(a) (b)

Fig. 6. (a) Wireless Communication block schematic; (b) Player block schematic.

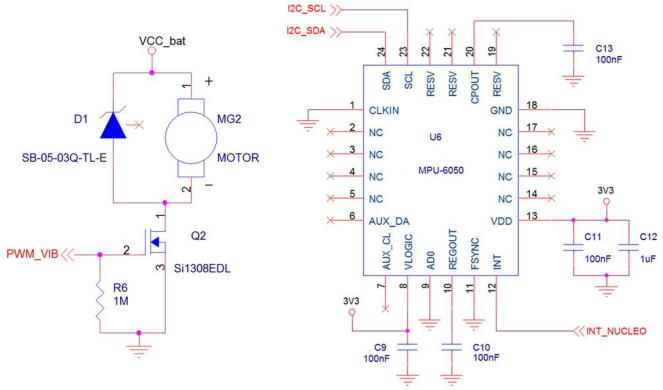

(a) (b)

Fig. 7. (a) Vibrator block schematic; (b) IMU block schematic.

The main characteristics of this component for which it was selected are that it has dimensions of 12×3 mm, an impedance of 8 Ω, and a nominal and maximum power of 0.5 W and 0.6 W, respectively.

4) Vibrator Block: In order to simulate the behavior of the chick inside the egg, slight vibrations must be generated. The caregiver at each request, which is made from the master system, adjusts the intensity and duration of the vibration. A small motor has been used which generates a vibration whose intensity depends on the applied input voltage. Since the microcontroller ports do not provide sufficient output current and, moreover, to protect the microcontroller, an N-channel MOSFET has been used, whose reference is Si1308EDL [35]. Fig. 7(a) shows the electrical schematic of the vibrator control circuit.

The MOSFET gate is controlled by a PWM output from the 303k8 core via the PWM_VIB signal. The MOSFET conducts if this signal is logic high and, due to its very low resistance between drain and source, a voltage of 3.3 V will be applied between the terminals of the motor winding, so that the motor will vibrate.

TABLE I
RELATION BETWEEN THE VOLTAGE APPLIED TO THE MOTOR AND THE CURRENT DRAWN.

Voltage (V)	Current (mA)
3.3	52.1
2	37.9
1.7	32.6
1.5	29.1
1.4	24.9
1.3	21.1
1.2	18.9
1	16.6
0.8	15.1
0.6	12.5

The SB-05-03Q clamping diode is connected in parallel with the motor to protect the MOSFET. This allows the high transient voltage induced in the motor coil to be quickly discharged when the MOSFET stops conducting.

The PWM output of the microcontroller controls the vibration power of the motor by varying the average voltage value between the terminals of the motor winding. The PWM output was programmed with a frequency of 10 KHz. The motor was experimentally characterized in the laboratory using the Agilent E3631A DC power supply and the Agilent 34401A multimeter, obtaining the voltage and current data shown in Table I.

5) Inertial Measurement Unit Block: The system has an IMU to monitor the movements of the egg performed by the bearded vulture. This monitoring is planned for future work, since the main objective of the work presented in this paper is to emulate a natural egg, and not to obtain incubation data that have been extensively studied in some works such as [23] and [24].

Fig. 7(b) shows the electrical schematic of this block, in which the main component is the MPU-6050 [36], which is a sensor based on MEMS (Micro Electro Mechanical Systems) technology. The MPU-6050 integrated circuit combines a 3-axis gyroscope, 3-axis accelerometer, and a DMP (Digital Motion Processor™) in a single package, making it a 6 DOF

(Degrees of Freedom) or a six axis IMU sensor. Additional features include an embedded temperature sensor and an on-chip oscillator with ± 1% variation over the operating temperature range.

The MPU-6050 incorporates a DMP (Digital Motion Processor) that reads data from accelerometers and gyroscopes and, from this data, executes motion processing algorithms. The microcontroller can read the processing results from the DMP registers or from an on-chip 1024 Byte FIFO buffer. The DMP and the FIFO buffer allow to reduce both the power consumption and the processing load of the microcontroller. The microcontroller can be in deepsleep mode while the MPU is acquiring data and, when the buffer is about to be full, the MPU will wake up the microcontroller by an interrupt (INT_NUCLEO, in our case). The microcontroller will read all the stored data from the MPU-6050 buffer, process it for its final application, and then return to deepsleep mode again.

Communication with all registers of the device is performed using either I^2C at 400 kHz via the I2C_SDA and I2C_SCL signals, which are connected to the I^2C bus of the microcontroller. The AD0 input pin allows to select its slave address on the I^2C bus. This pin has been connected at logic low level, as can be seen in Fig. 7(b), so its address will be 68_{16}.

The Full-Chip Idle Mode Supply Current is only 50 μA and the Normal Operating Current with Gyroscope, Accelerometer and DMP activated is 3.9 mA. Because of its low power consumption and since it operates from power supply voltage range of 2.375 V-3.46 V, its power supply pin, VDD, has been connected to the output of the main regulator, U8 (as shown in Fig. 7(b)), which generates the 3.3 VDC supply voltage of the microcontroller.

6) Temperature and Humidity Sensor Block: As indicated above, a sensor for measuring temperature and relative humidity has been included inside the egg. The SHT31-DIS_B sensor [37], which is the standard version of the SHT3X series of sensors, is used. The SHT3x-DIS has increased intelligence, reliability and improved accuracy specifications compared to its predecessor due to Sensirion's CMOSens® technology. This sensor is capable of measuring relative humidity values in the range of 0% to 100% RH with an accuracy of ± 2% RH and a resolution of 0.01% RH. Regarding temperature, the measuring range varies between 0 and 90 °C with an accuracy of ± 0.2 °C and a resolution of 0.01 °C. The SHT31-DIS_B sensor is connected to the microcontroller via the I^2C bus as well as the IMU, MPU-6502. Its functionality includes enhanced signal processing and two distinctive and user selectable I^2C addresses (44_{16} or 45_{16}) that allow two sensors to be connected to the same I^2C bus.

The SHT31-DIS will be used in single shot mode, because the temperature will only be sent when the master wakes up the slave system, and sends a command to request the temperature value. In single shot mode, the SHT31 has a maximum idle state power consumption of 2 μA and 1.5 mA while measuring, and typical values of 0.2 μA and 0.6 mA, respectively. Sensirion specifies a typical average power consumption in the order of 1.7 μA, considering that a measurement is performed every second and using the single shot mode. Therefore, in our system the power consumption will be lower, since the expected measurement frequency will be in the order of 300 times lower and since it can be power supplied with a range of 2.15-5.5 V, it has been connected directly to the 3.3 VDC supply voltage generated by the main regulator U8 (as shown in Fig. 8(a)).

A breakout board [38], which includes the SHT31-DIS_B sensor, has been used instead of soldering it directly on the PCB, since this way it can be placed in any area of the egg. This will allow temperature and humidity measurements to be taken anywhere on the egg, such as the inner side of the shell. Therefore, a 4-pin male connector has been included on the PCB where the I^2C bus of the microcontroller is accessible, and where the breakout board with the SHT31-DIS_B sensor will be connected.

7) Power Supply Block: Fig. 8 shows the electrical schematic of the power supply block. The power supply voltage of the system is obtained from a rechargeable li-ion battery that is connected to connector J1. Specifically, the battery used for the tests has been Samsung INR21700-50E [39]. Among the most remarkable features of this battery are that it has a nominal and maximum voltage of 3.6 V and 4.2 V, respectively. Currently there are batteries in the 18650 and 21700 formats with a higher capacity, which could also be used.

The design also includes two MIC5503-3.3YM5 voltage regulators [40] to generate a voltage of 3.3 V from the battery voltage, as shown in Fig. 8(a) and (c). The U2 regulator generates the supply voltage of 3.3 V for the Nucleo-303k8 board, the accelerometer and the vibrator, and the U3 regulator the supply voltage of 3.3 V to the XBee module. These regulators are of LDO (Low DropOut) type. Dropout voltage, V_{DO}, which gives these regulators their name, refers to the minimum voltage differential that the input voltage, V_{IN}, must maintain above the desired output voltage, V_{OUT}, for proper regulation. Any LDO has a much lower V_{DO} than the classic linear regulators. Specifically, the MIC5503-3.3YM5 has a very low V_{DO} (160 mV at 300 mA output current), so it guarantees a regulated output voltage of 3.3 V for a battery voltage of only 3.46 V, as shown in Equation (1).

$$V_{IN} \geq V_{OUT} + V_{DO} \tag{1}$$

Another advantage of an LDO is that if V_{IN} is lower than the value calculated by Equation (1), in our case 3.46 V, the regulator keeps working, although it no longer generates a regulated voltage at its output, but depends on the input voltage, and would be determined by Equation (2):

$$V_{OUT} = V_{IN} - V_{DO} \tag{2}$$

Therefore, it could still power the Nucleo 303k8 and XBee module, since they can operate with voltages lower than 3.3 V. In this way the embedded system will be able to operate up to a battery voltage of 3.3 V, which is the minimum supply voltage of the DFPlayer module. If the battery voltage drops below this value, the entire system will go into deepsleep mode.

A very important characteristic to consider when selecting an LDO is the quiescent current, which is usually represented by I_Q. The quiescent current is the current drawn by a system

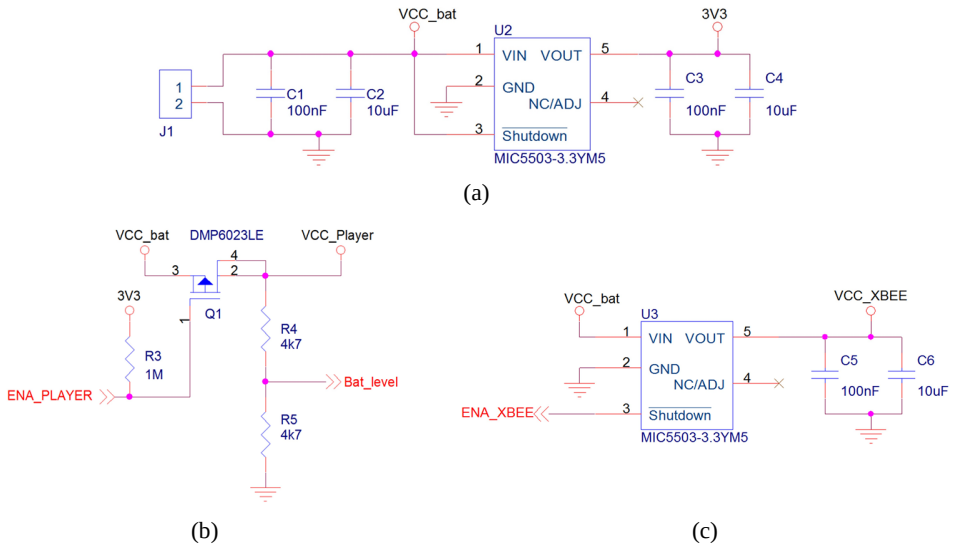

Fig. 8. (a) 3.3 V power supply schematic; (b) Player power control schematic; (c) XBee module power supply schematic.

in standby mode with light or no load. Equation (3) determines the power dissipation, P_D, of an LDO, where I_{OUT} is the current drawn by all loads connected to its output.

$$P_D = (V_{IN} - V_{OUT}) \times I_{OUT} + V_{IN} \times I_Q \tag{3}$$

If the loads are not in standby mode, the power consumption will be determined primarily by the load (I_{OUT}), but if all the circuits powered by the LDO are in standby mode, quiescent current (I_Q) plays a much greater role in the power dissipated. Since our system will be in sleep mode most of the time, the LDO MIC5503-3.3YM5 has been selected, since it has an I_Q of only 38 μA, which means a quiescent power of only 0.137 mW, considering that V_{IN} is the nominal voltage of the battery (3.6 V).

One way to conserve battery life is to put in shutdown mode the regulators that feed the modules that are going to be in standby mode, such as the XBee module. If the Shutdown pin of the LDO U3 (see Fig. 8(c)) is set to logic low, it will shut down its output. The shutdown current of MIC5503-3.3YM5 is lower than its quiescent current, specifically its typical value is 50 nA. When the power to the XBee module is interrupted, it can consume current through its reception pin. To reduce this current to 0 μA, it is necessary to configure the microcontroller's serial transmission pin (XBEE_TXD) as a pull-down input, returning to the initial configuration when the XBee module is supplied.

To reduce power consumption as much as possible, a MOSFET (6023LE model) [41] has been chosen to manage the power supply of the MP3 player so that it does not consume when no sounds are being played. Fig. 8(b) shows the electrical schematic of the DFPLAYER power supply control circuit. A MOSFET has been used instead of an LDO because it guarantees the operation of the DFPLAYER up to a voltage of 3.3 V from the battery, since it does not need a minimum input voltage like an LDO. The power supply is controlled by the ENA_PLAYER signal which is connected to the PA_4 port of the microcontroller. When the ENA_PLAYER signal is at high logic level, the power supply is interrupted and when it is at low logic level, the DFPLAYER module is power supplied. When the transistor cuts the power to the DFPLAYER, the module may continue consuming current through the microcontroller's serial transmission pin (PLAYER_TXD). To reduce to 0 μA the current consumed by the reception pin of the DFPLAYER module, it is necessary to configure the microcontroller's serial transmission pin as pull-down input, and return to its initial configuration when the DFPLAYER module is supplied.

As shown in Fig. 8(b) and (c), the power supply to the XBee and DFPlayer modules is controlled using the ENA_XBEE and ENA_PLAYER signals, which are connected to PA_1 and PA_4 pins of the microcontroller, respectively. When the microcontroller is in deepsleep mode, these ports are set to high impedance, so it is necessary to set the appropriate shutdown value on each signal using two resistors. U3 LDO is shutdown when ENA_XBEE is at low logic level, so a pull-down resistor must be connected to PA_1. However, it is not necessary to add this resistor, since the MIC5503-3.3YM5 includes an internal pull-down resistor with a value of 4 MΩ, so the input current is less than 1 μA (the manufacturer specifies a typical value of 50 nA). This is another reason why this LDO has been used. The DFPlayer module is deactivated when ENA_PLAYER is at high logic level, so pull-up resistor R3 is connected to 3.3 V so that the V_{GS} voltage of the MOSFET-P is higher than its threshold voltage and therefore does not conduct.

To ensure system operation, the battery charge level must be monitored by analyzing its voltage value using one of the two Analog Digital Converters (ADCs) in the microcontroller. Since the battery voltage can be up to 4.2 V when fully charged, its voltage value must be reduced in the range of 0 V to 3.3 V of the ADC. To do this, the voltage divider consisting of the two resistors, R4 and R5, is used as shown in Fig. 8(b). Since both have the same value and this is much smaller than the input impedance of the ADC channel, the output

voltage of the divider, Bat_{-level}, will be given by Equation (4). Therefore, the maximum value of Bat_{-level} will be 2.1 V.

$$Bat_{-level} = \frac{V_{CC-bat}}{2} \tag{4}$$

It should be noted that if the resistive divider had been connected directly to the battery output, it would result in a permanent current consumption of 383 μA, as shown in Equation (5), considering an average battery voltage value of 3.6 V. As it is not necessary to continuously monitor the battery charge level, the voltage divider has been connected to the supply voltage of the DFPlayer module. In this way the average I_{DIV} value is reduced to almost 0 μA, since the MOSFET-P, Q1, will only be in conduction if the battery level is to be measured or sounds are to be played by the MP3 player.

$$I_{DIV} = \frac{V_{CC-bat}}{R13 + R14} = \frac{3.6V}{4K7 + 4K7} = 383\mu A \tag{5}$$

B. Power Consumption and Savings Strategies

One of the most important challenges of an active egg is to achieve the longest possible autonomy, to avoid inconvenience to the bird when changing the battery. The aim is to reduce the frequency with which the egg has to be replaced by another one. The capacity of the battery and the power consumption of the components chosen are decisive. By improving both, we can increase the battery life in successive prototypes. However, there are other factors that, once the system components have been chosen, have an impact on battery life, which we will discuss below.

Three strategies have been followed to increase the autonomy of the system, although it should be noted that the autonomy will depend on the frequency and intensity of the physical actions of the egg. One strategy, at the hardware level, has consisted of a careful design of the power block to reduce power consumption. This block has been described in detail in section II-A.7. The second strategy, at the software level, has been that only the peripherals involved in a caregiver request are powered in the egg, and only for as long as necessary. The third strategy has consisted of studying whether it is possible to keep the egg asleep for certain intervals without affecting the functionality of the system, while maintaining the requirement that the caregiver must have real-time control of the egg when it excites the bird. For this purpose, it has been necessary to observe the operations performed by the caregiver during the first tests. Studying the operations suggested by the caregiver, the egg is activated with a very low periodicity around 30 minutes and the movements and sounds are usually planned. The strategy of putting the egg to sleep in certain periods must satisfy the requirement that the physical actions of the egg must be performed under request and supervision of the caregiver, and that the egg cannot perform physical actions autonomously.

Table II shows the average current consumption of the egg under certain conditions depending on the peripheral being powered. The data have been obtained in the laboratory with the Agilent 34401A multimeter and the Agilent E3631A DC power supply.

The table does not show the power consumption values when the egg transmits, which, although of short duration, are high. However, it does not influence in the following discussions on power consumption saving strategy.

To carry out any action, the egg is waiting for a command from the master for which the Nucleo and the XBEE module must be active. In this case the average consumption is 46.26 mA. If the egg could be kept in deepsleep mode indefinitely, its consumption would be reduced by 0.071 mA and the autonomy with the same battery would increase enormously.

Putting the egg in deepsleep mode indefinitely and waking it up only when it is needed to attend to the master would be the ideal situation to achieve sufficient autonomy to cover the entire incubation period (which, in the case of the bearded vulture, is 54 days). However, this is not possible because the communications module must be powered to receive commands from the master.

As already mentioned, the caregiver requests physical actions from the egg with a very low periodicity. In addition, and most importantly, it is not necessary to have permanently active communication (on-line) between the egg and the master, to give an immediate answer when the caregiver decides to activate it, but it is possible to delay the activation. Under these conditions, it has been decided that the egg should remain asleep and wake up from time to time to check if there are any requests from the caregiver. The consequence of this strategy is that the caregiver must wait for the egg to wake up in order to excite the bird. In return, a significant saving in power consumption is achieved. Logically, the application in the master will be performing retries waiting to coincide with a period of awake egg and from there, the caregiver can request actions to the egg. Once the egg wakes up, it remains in this state as long as it is receiving requests from the caregiver. A maximum inactivity time has been established and after this time the egg goes back to sleep, if no other action has been requested. This strategy increases the autonomy of the egg, which is always kept on-line.

In conclusion, during one time interval the egg remains asleep and will consume 0.071 mA and during the other time interval it remains awake and consumes 46.26 mA. If the caregiver also makes a request, there will be some punctual consumptions according to Table II. With the awake/sleep strategy the battery life will depend on this ratio. The duration of the initialization functions of the system has been studied and it has been concluded that a time of 15 seconds awake is more than enough to start attending the requests of the master. Therefore, the egg will wake up for 15 seconds and if it does not receive a request, it can go back to sleep. The sleeping time has been set at a maximum of 105 seconds, since the caregivers have considered that this would be an acceptable waiting time for the egg to perform an action.

Another variable that influences consumption using the awake/sleep strategy is the maximum inactivity time, which is the maximum time that the egg is active without performing any physical action or communicating with the master. Once the maximum inactivity time is exceeded, the egg goes to sleep

TABLE II
LABORATORY TEST OF THE CURRENT CONSUMPTION OF THE EGG POWERED WITH A BATTERY VOLTAGE OF 4.2 V.

Conditions	Current (mA)
Egg sleeping (Nucleo sleeping) peripherals OFF	0.071
Control Unit (Nucleo) Normal operation + XBEE module reception	46.26
Egg Vibrating 100% (Nucleo+Vibrator+XBEE reception)	109.2
Playing sound at maximum volume (Nucleo+Player+XBEE reception)	110.3
Egg Vibrating 100 % and playing sound at maximum volume (Nucleo+Player+Vibrator+XBEE reception)	165.4

and will continue the awake/sleep cycle. This time would be very small if, after exciting the egg, the caregiver immediately puts the egg to sleep from the application. However, the caregiver should wait to see the bird's reaction and decide if further actions should be taken. An inactivity time of 120 seconds has been set, since this is the maximum reasonable time in the awake/sleep cycle. It should be noted that this time influences current consumption differently depending on the awake/sleep ratio and, of course, the number of times that the egg is excited.

To verify this in more detail, let us consider that the current consumption, depending on how long the egg is in an inactive state, awake, asleep, or playing sound/vibrating, during a total sampling time t_{ts}, would be determined by the following equation:

$$I_{Dts} = I_i d \cdot \frac{t_{id}}{t_{ts}} + I_{aw} \cdot \frac{t_{aw}}{t_{ts}} + I_{sl} \cdot \frac{t_{sl}}{t_{ts}} + I_{rsv} \cdot \frac{t_{rsv}}{t_{ts}} \quad (6)$$

with $t_{ts} = t_{id}+t_{aw}+t_{sl}+t_{rsv}$; where I_{id} is the consumption of the egg in the inactive state; t_{id} the time in the inactive state; I_{aw} the consumption in the awake state; t_{aw} the time in the awake state; I_{sl} the consumption in the sleep state; t_{sl} the time in the sleeping state; I_{rsv} the consumption while reproducing sound and vibrating; and t_{rsv} the time in the reproducing sound and vibrating state.

Considering Equation (6) and a battery with an accumulated energy of 4259 mAh (the reason for this particular value will be determined in the results section), the battery life can be calculated for different ratios between awake and asleep states, as well as for different values of idle state time. The different results obtained can be seen in Fig. 9.

The calculations have been performed taking into account a total sampling time t_{ts} of one hour and an excitation period of ten minutes, in which a one-second vibration and sound are produced for ten seconds at maximum volume. As can be seen in the figure, this time has practically no influence on battery life if the awake time is similar to the asleep time, but it has a decisive influence if the asleep time is longer than the awake time.

C. Communication Protocol Design

A safe and reliable communication system has been developed between the master and slave subsystems. The master sends requests to the slave, and the slave can only send messages in answer to the requests of the master. To ensure that each master communicates with its slave, a protocol has been designed whose message format is shown in Fig. 10. Although, as already mentioned, to avoid errors in the selection of the slave by the caregiver, currently the communication configured in the XBEE is point-to-point, from a single master to a single slave. This message consists of 263 bytes at most, and its format includes the service, origin and final destination of the message to ensure that messages are sent and received from the correct device. The other fields consist of Length, Data and CRC. Data field includes the information to be processed by the application and has a maximum size of 255 bytes. Two different formats have been developed for Data field that are request and request answer. The length of Data field is provided in Length field. Finally, CRC field includes the result of adding each byte of the message, and is used to check whether the message was successfully received.

The purpose of request messages is to indicate to the slave that an order must be invoked. The format of these messages is shown in Fig. 11. Seq field (1 byte) represents the sequence number that uniquely identifies the request and is used to control that the same request cannot be executed multiple times. Cmd field (1 byte) is the identifier of the order that is requested to be invocated. If the order requested is an action, status field (1 byte) indicates whether the action is to be started or stopped. Finally, the message is composed of the attributes of the order that are included in Arguments field (0-253 bytes).

The slave answers each request message with a reply message indicating whether or not an error was detected. If the master requests information from the system or sensors, the answer message may also contain this type of information. Fig. 12 illustrates the syntax of the answer messages. Seq field (1 byte) represents the sequence message that identifies the request message that is being replied to. The identifier of the requested order is indicated in Cmd field (1 byte). If the request was for initiation or stopping is indicated in status (1 byte). If an error has happened, res field (2 bytes) will include ASCII ER characters; and if the request has been successful, OK character will be included. The message also includes 4 bytes to represent the error code. Finally, since some orders return information, data field (0-247 bytes) includes the answer data.

D. Design of the Software for the Master System

The master software runs on a general-purpose computer, under Windows operating system. An XBee Series 1 module must be connected to the general-purpose computer where the master software is installed in order to be able to communicate with the slave. The Digi XBee-USB adapter board, which provides a simple interface between PC and XBee, has been used for this purpose [26].

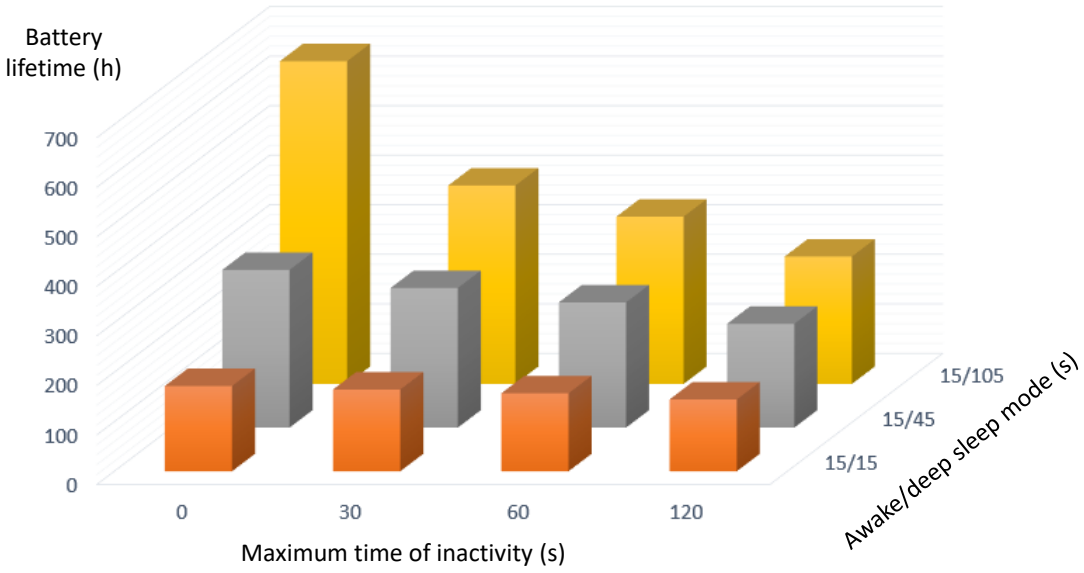

Fig. 9. Influence of maximum idle time on battery life according to awake/sleep ratio.

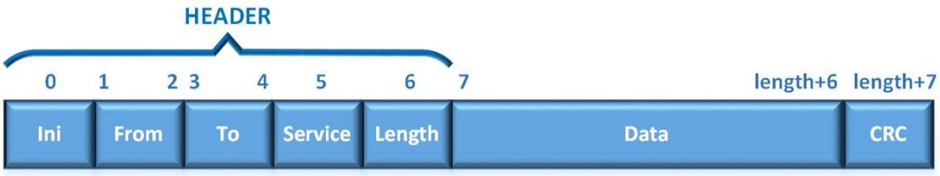

Fig. 10. Message format.

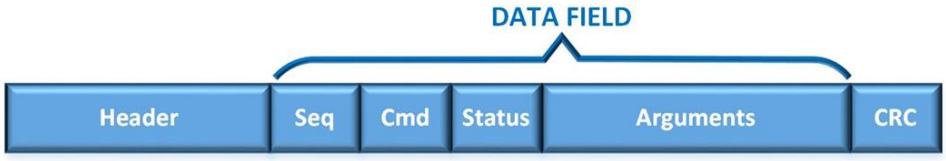

Fig. 11. Data payload Request message format.

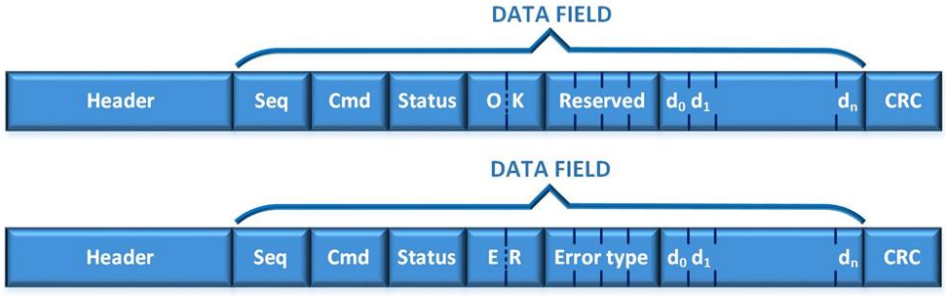

Fig. 12. Data payload Answer message format.

The master system interacts with the user (through a graphical interface) to provide the caregiver user with the ability to control the embedded system. The interface translates user commands into messages, which are sent to the slave. The actions that the user can perform are to start/stop vibration, start/stop reproduction and request status. The interface consists of several windows (Fig. 13) which can be accessed by selecting the different menu buttons. In Fig. 13(a) there is a configuration window showing a list of available serial ports, from which the user can select the serial communication port to which the XBee module is connected. The field labeled as Available Tracks receives a numeric value and must be

filled with the number of songs loaded on the microSD card of the DFPlayer module. Fig. 13(b) and (c) illustrate the windows for starting/stopping a vibration or reproduction of sounds. As shown in the figure these windows include fields for selecting the duration and intensity of the vibration as well as the list of sounds to be displayed and the volume. Finally, Fig. 13(d) shows the window that appears when the option of checking the status of the slave system is selected. As it can be seen this window includes as information whether the egg is reproducing sounds or vibrating and the battery charge percentage values as well as the percentage of humidity and temperature inside the egg. Each time the user requests the execution of an action, the graphical interface displays a success or error message depending on whether or not it has been successfully executed. In the event of an error, it displays a code indicating the causes of the error.

All requests sent to the slave are performed using the same procedure. A message is created with the corresponding sequence number and sent to the slave. The master waits a certain amount of time for a reply. If an answer is received from the slave with the same sequence number included in the sent message, it confirms that the message has reached the slave and has been attended to by the slave. In this case, the sending process is finished and the sequence number for the next message to be sent is increased. In the event that no answer is received, or the answer is incorrect (e.g. if a reply arrives with a different sequence number than the message sent), a series of retries are carried out, all with the same sequence number, until a correct answer is received, or the maximum number of retries is reached. Using the sequence number, a mechanism has been designed to detect repeated orders. For each order, the sequence number of the last message that executed it successfully is stored. In this way, when a new message arrives at the slave, it is checked whether the sequence number is the same as the last message that successfully executed that order, and if it is, it is discarded.

In order to store a record of communications between the master and the slave, the application running on the master generates two types of log files in spreadsheet format. One of the files stores the record of requests from the master and answers from the slave, indicating whether these have been successful or whether an error has happened, while the other stores the status information received from the slave when the slave is requested for its status.

E. Design of the Software for the Slave System

The slave system software runs on the STM32F303K8 microcontroller included in the F303K8 Core development board. The necessary software has been designed to ensure that the embedded system provides the functionality to reproduce sounds, perform vibrations, communicate wirelessly and perform humidity and temperature measurements.

All the software running on the egg has been developed, including the firmware that manages the peripherals. In this sense, two USART peripherals of the microcontroller were used to operate the XBee module and the DFPlayer module for which it was necessary to implement two FIFO software queues. On the other hand, a PWM signal has been generated to control the vibration power. For the measurement of the battery charge level, one of the four analog-to-digital converters of the microcontroller was used. As the maximum battery voltage is 4.2 V and the microcontroller operates at 3.3 V, the input voltage on the pin connected to the converter has to be adapted using a voltage divider.

As discussed in section II-B, in order to maximize battery life, it has been decided that the egg should operate on an awake/sleep cycle. When the caregiver wants to activate the egg, it will have to wait, in the worst case, the time that the egg is asleep, after which it will stay awake as long as commands are being sent. A maximum inactivity waiting time is provided for a new command, after which the egg goes back to the awake/sleep cycle. The awake/sleep time is not fixed, but can be adjusted by the caregiver, although in these early tests it has been fixed to avoid errors that would make impossible to wake the egg.

The system can be in two operating modes, normal mode or deepsleep mode. The deepsleep mode is a low power consumption mode in which all the microcontroller peripherals are switched off except the RTC, which is in charge of waking up the system after a preset time. When the system wakes up, it waits for a time to receive a message from the master requesting that it wakes up. If this message is received, the system switches to normal mode, otherwise it goes back to sleep. Fig. 14 shows the activity diagram of the system when it is in deepsleep mode. The system can be in this mode if the battery voltage value is less than 3.3 V; in this case the system returns to deepsleep mode by deactivating the RTC so that it does not wake up again. The microcontroller also switches into this mode if the maximum idle time is exceeded and the caregiver has not commanded the egg to go into sleep mode.

The activity diagram in Fig. 15 shows the execution process when the system is in normal mode.

The egg executes commands that can be of two types: information request (this does not perform any physical action) or start/stop an action. For each command implemented it is necessary to keep the following information: whether it is being executed, type of command, the instant at which the last execution was started, the instant at which the execution must be stopped, the sequence number of the message that executed it, a command identifier and a callback to the function that implements the actions to be performed. All this information is kept in an array of structures so that the status of each command will be available in one position of the array as shown in Fig. 16. From each new message received by the egg, among other parameters, the command identifier is extracted, which is used to locate the position of the structure, which is modified according to the message received.

Although no operating system has been integrated into the egg software, there is a periodic real-time interrupt associated with the SYSTICK timer of the ARM Cortex-M4 core, as a tick. Tick is implemented through a special 24-bit countdown timer. It is configured to generate an interrupt every millisecond. On each tick, the system reads the status information of each command, checking if there is any action to perform and calling the function that performs it, using the callback

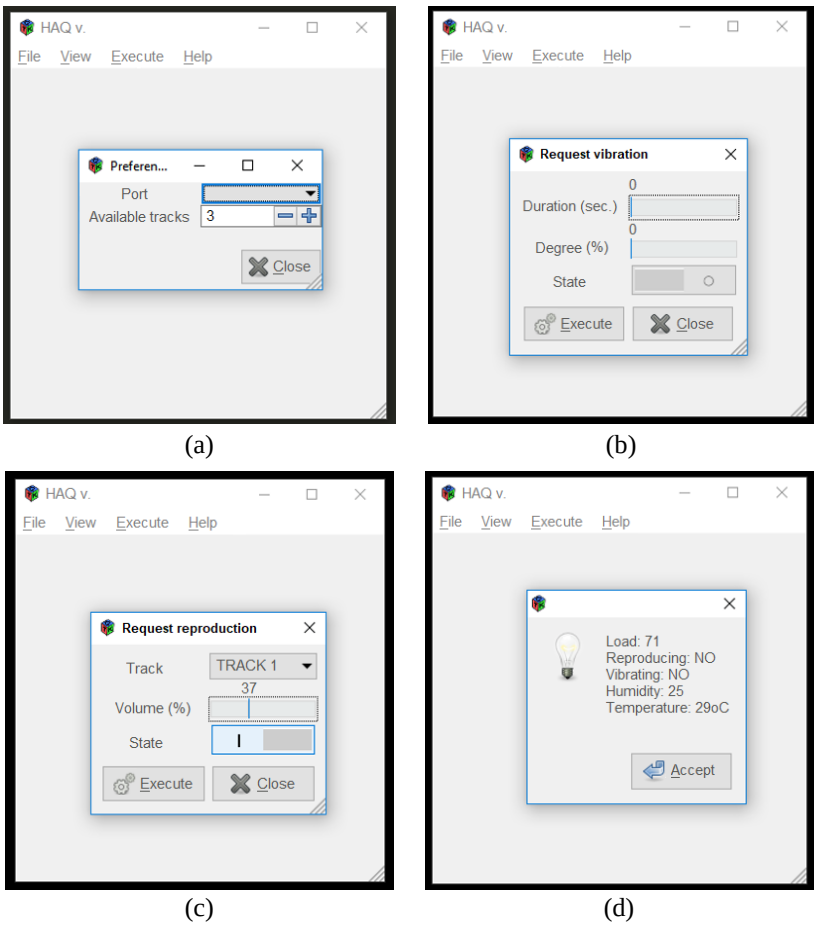

Fig. 13. (a) Configuration window; (b) Window for starting/stopping a vibration; (c) Window for reproduction of sounds; (d) Status window.

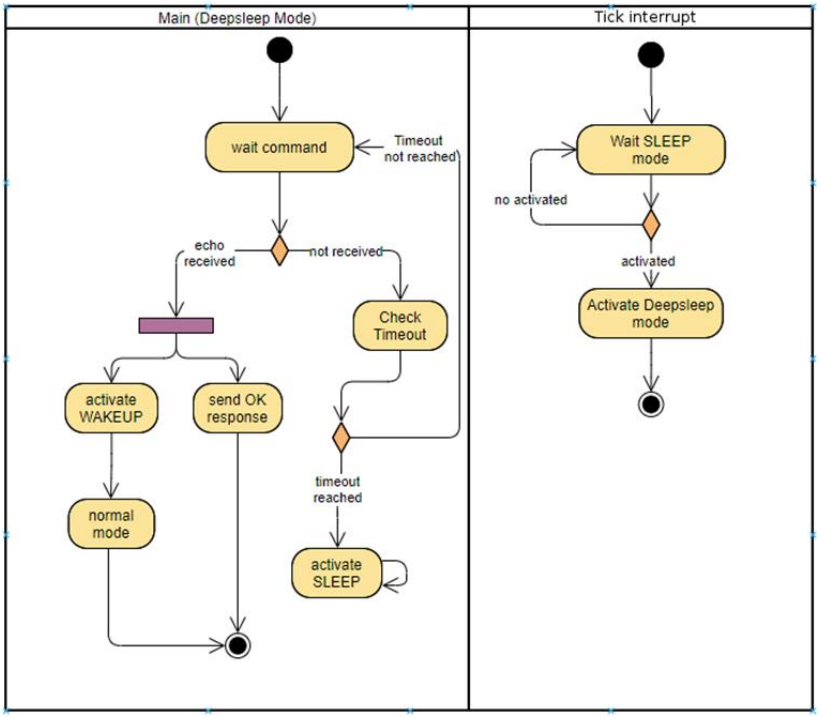

Fig. 14. Activity diagram of the system in deepsleep mode.

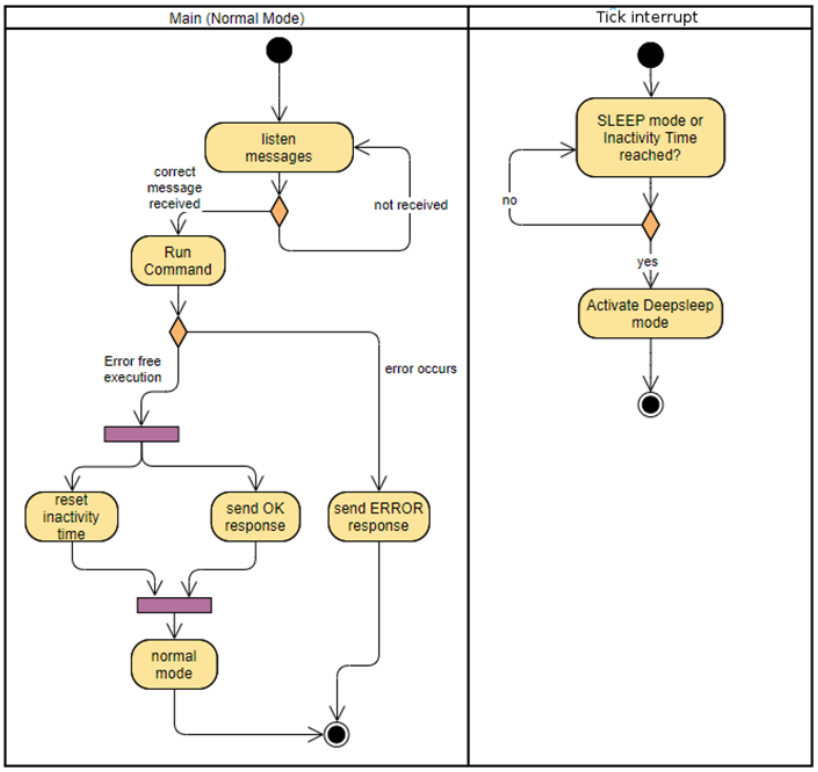

Fig. 15. Activity diagram of the system in normal mode.

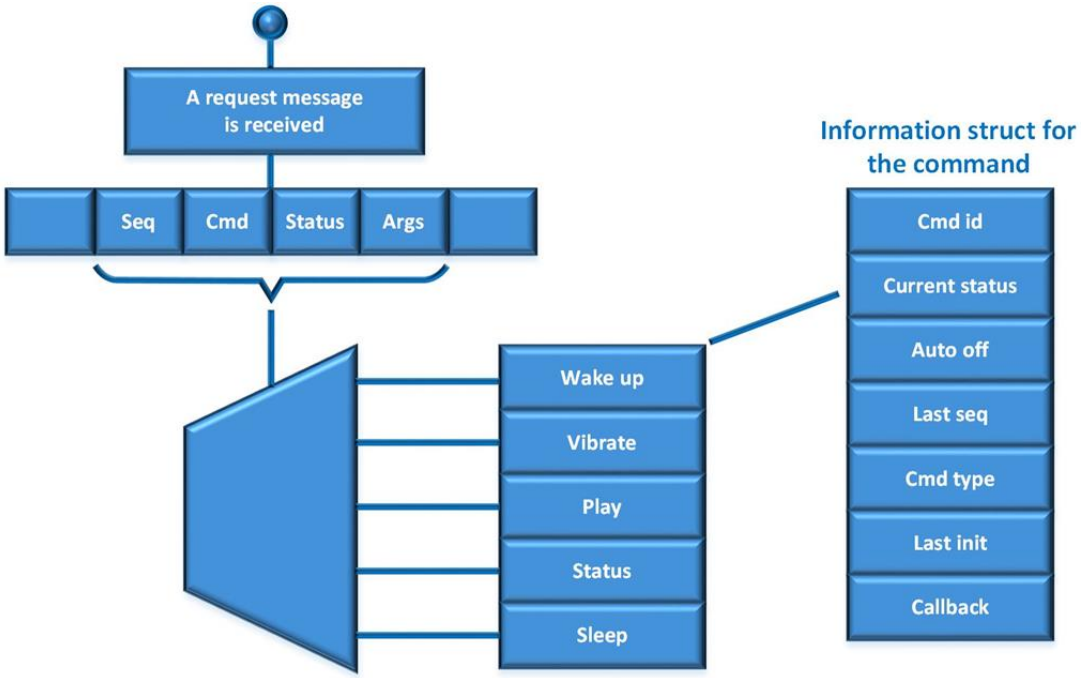

Fig. 16. System image scheme.

available in the command structure and updating the command structure with the new status information. The tick is in charge of managing the input to the deepsleep mode, handling the stop of orders with a maximum operating time and monitoring the status of the DFPlayer module to disconnect it when it is not playing sounds. Finally, the calendar clock has been configured to be able to take the microcontroller out of the deepsleep low-power mode.

III. Results

This section describes the tests carried out to check the correct operation of the developed device, the verification of

the autonomy calculated theoretically in section II-B, and the real operating tests in the nest.

A series of lab tests have been carried out to verify that the embedded system works as expected and satisfies the requirements. All the tests carried out have given a satisfactory result, thus demonstrating that the elements that compose the system are compatible, that they interact correctly and that they transfer the correct data at the right time through their interfaces.

In addition, a test was carried out to obtain the maximum transmission distance. As in real operation the master system will be in a house, separated by a maximum distance of 30 m from the bird's nest, the master was placed in our laboratory and the slave was moved along a corridor. According to this test, the communication between master and slave worked correctly up to a distance of approximately 120 m. Therefore, in the real situation the communication should work properly, because the distance is smaller and, once the signal crosses the wall of the house, there is no obstacle between the house and the nest that could reduce the signal level.

Another important aspect is to know the discharge curve of the battery up to a voltage of 3.3 V, which is the voltage value at which the system definitively switches to sleep mode. This will also allow us to compare the theoretical results with the laboratory tests and to determine the autonomy of the battery in the different cases considered. This curve is not available in the battery datasheets and, moreover, even if it were available, it could vary depending on the average discharge current. For this reason, a discharge test was carried out in the laboratory to obtain the voltage drop curve in function of time. For this purpose, a constant current source and a microcontroller have been connected to the battery to monitor the battery voltage value and store it on a microSD memory card in Excel format. A value of 93.4 mA has been selected for the constant discharge current, because this value is very close to the average current consumption of the system when it is awake. Fig. 17 shows the discharge graph of Samsung INR21700-50F battery. The manufacturer specifies that the minimum discharge voltage of the battery is 2.5 V, so, according to the curve, this voltage value is reached after 53 hours of discharge. From the curve it can be concluded that, although the manufacturer indicates that the battery capacity is 5000 mAh, it has a real value of 4941 mAh, but for the minimum discharge voltage (2.5 V), as can be seen in Equation (7):

$$C_B = 93.4mA \cdot 52.8h = 4940.86mAh \tag{7}$$

where C_B is the battery capacity.

On the other hand, since our system definitely switches to deepsleep mode if the supply power is less than 3.3 V, the real operating capacity of the battery would be 4260 mAh, approximately, as is shown in Equation (8):

$$C_{BP} = 93.4mA \cdot 45.6h = 4259.02mAh \tag{8}$$

Where C_{BP} is the performance of the battery capacity.

Fig. 18 shows the battery life with different awake/sleep periods in the tests developed in the laboratory. Actions are performed every 10 minutes which include a 1 second vibration at maximum power and sound playback at maximum volume for 10 seconds. The data has been obtained in the laboratory using the ADC of the STM32F303K8 to obtain the battery voltage and send it to the master, which stores it. The egg is powered by a Samsung INR21700-50E 5000 mAh – 10 A battery. These actions are those suggested by the caregivers, but these are performed more frequently than in the real tests. In the real tests, the specific actions will depend on the reactions of the bird and the caregiver will decide whether to continue the vibration, the sound or both for a longer period of time or to perform them more times. Given the lack of experience with this type of eggs it is difficult to decide the correct pattern. As it can be seen from Fig. 18, a battery lifetime between 133.9 and 255.6 hours has been achieved. During the last season the egg was programmed with an awake/sleep period of 15/105 to have a higher autonomy, without any operational problems.

The tests on the birds were carried out in 3 seasons (2018, 2019 and 2020) and were performed with a foster male and a natural pair. In all cases it has been observed that the birds accept the artificial egg by reacting appropriately to the activation of the vibration, and exhibiting an identical behaviour to the movement caused by a chick in a natural egg. In fact, it was observed that the activation of the vibration was the most stimulating for the birds. About the reproduction of sound, only in one case the bird listened to the sound because the bird was up from incubation and showed interest in the sound, just as he would have done if he had heard the sound of a chick in a natural egg. The fact that the birds did not react when the sound was produced while they were incubating the artificial egg leads us to think that they did not hear it when it was under their bodies. The thickness of the egg shell to ensure its strength and the limited power of the MP3 player to reduce the power consumption of the system may be the cause of the absence of stimulus in the foster male by not hearing the sound.

In the real tests carried out on the birds in the Bearded Vulture Breeding Unit of the Vallcalent Wildlife Centre, actions were programmed every 30 minutes by exposing the foster male to vibration for one second and sound emission for ten seconds at maximum power. An awake/sleep ratio of 15 seconds and 105 seconds respectively was programmed and an egg battery life of 8 to 10 days was achieved depending on the performance of the caregiver by repeating the actions.

IV. Conclusions

This work has presented an active artificial egg for the bearded vulture (Gypaetus barbatus), a bird in the process of recovery in Europe thanks to different reintroduction projects led by the Vulture Conservation Foundation (VCF), which require captive breeding of specimens to be released.

A small device has been developed that can be placed inside an artificial egg. Compared to other prototypes described in the literature, this device not only captures humidity and temperature data but is also capable of imitating the behavior of a natural egg in hatching, generating vibrations and sounds.

The software for this prototype has been developed, which executes the received orders. A graphical interface that sends

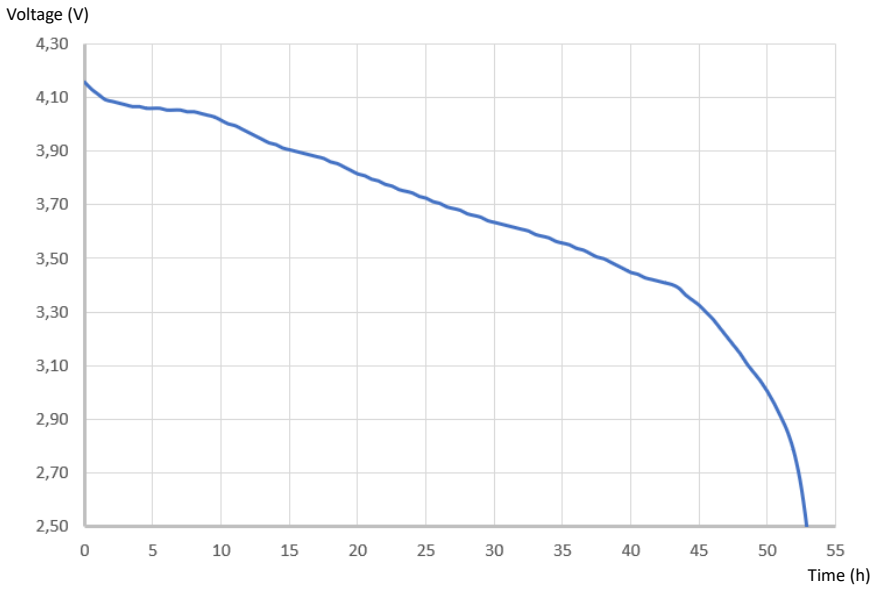

Fig. 17. Discharge curve of Samsung INR21700-50E battery.

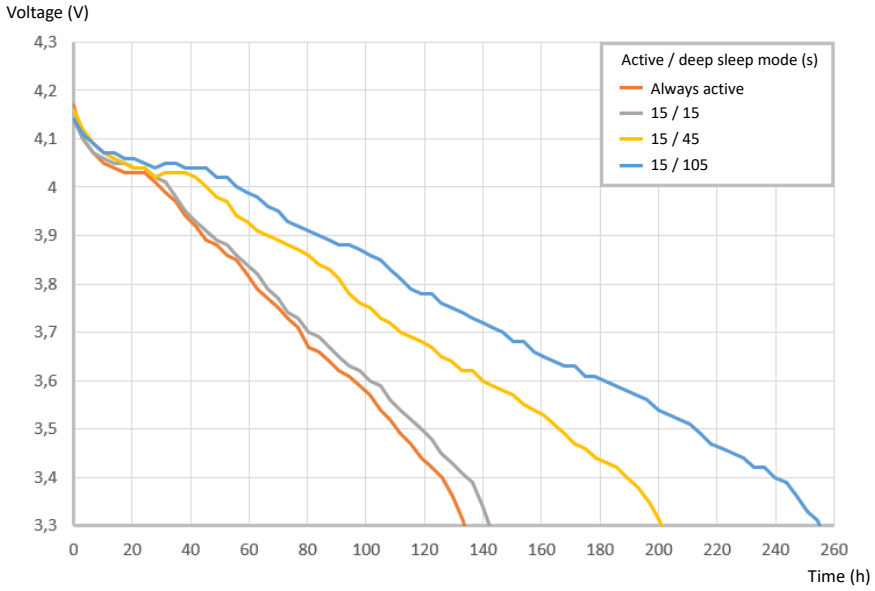

Fig. 18. Battery life in function of the awake/sleep period.

the orders remotely on request to the user was also designed, and therefore, a communication protocol that allows messages to be exchanged between the prototype and the desktop application in a secure way.

On the other hand, it has been possible to develop an embedded system with good autonomy. To achieve this, it was necessary to minimize power consumption by using the microcontroller's deepsleep mode and managing the power supply of the communication module and MP3 player. For the communication module a LDO voltage regulator with a very low quiescent current has been used and for the control of the MP3 Player power supply, a P-channel MOSFET has been employed, so that it has been achieved that the system does not definitely switch to deepsleep mode until the battery voltage is not equal to 3.3 V. This minimum value is fixed by the minimum supply voltage of the MP3 player (3.2 V), and because it is not advisable to discharge the battery to a value lower than this, since the autonomy is not greatly increased, but the useful life of the battery can be reduced by discharging it too much.

Moreover, a theoretical study was carried out to deduce the ideal strategy to increase the autonomy of the system. This study proposes different ratios between awake and asleep states. From this theoretical study it can be concluded that if the ratio is 15/15, autonomy remains practically constant even if the time of inactivity increases. However, if the time spent asleep increases in relation to the awake time, autonomy increases. Since the caregiver specified that the maximum

waiting time for the egg to answer to his commands was 120 seconds, the ideal ratio was considered to be 15/105. In this way, the autonomy of the system is 257 hours. In order to verify the veracity of the results of the theoretical study, a series of tests were carried out in the laboratory under the same conditions. The results of these tests verify that the real autonomy values are very close to the theoretical ones. Specifically, using an awake/asleep ratio of 15/105, the real autonomy value is 255.6 hours. This data is also close to those obtained in real tests with the bird, in which the autonomy varied between 8 and 10 days. It should be noted that the autonomy of the egg will vary depending on the commands sent by the caregiver, because vibration and sound reproduction have a high power consumption.

In the current system it is easy to implement pre-programmed actions of the egg, but as discussed throughout the paper, these have been discarded in favor of real-time control by the caregiver given the lack of experience with the reactions of the bird.

The artificial egg has been successfully tested with the bird for three seasons. Due to the fact that the developed egg vibrates and emits sounds such as a real one, the bird has not rejected the egg, achieving one of the proposed objectives of the work.

The size of the system, and thus of the egg, could be reduced for other endangered birds by using, in addition to the Wireless module, the STM32F303K8 microcontroller, a microSD memory card and a small power amplifier. This could also increase the sound reproduction power and further reduce the power consumption.

Although the current prototype has an acceptable autonomy, it could be increased by using other wireless communications modules with lower power consumption. For example, the LORA SX1272 module from Libelium [42] with the SX1272 transceiver [43] can be used, whose pinout is compatible with the Digi XBee SX 868 module, which is currently used in the egg.

ACKNOWLEDGMENT

The authors would like to thank the Bearded Vulture Breeding Unit of the Centro de recuperación de fauna salvaje de Vallcalent of the Generalitat Catalana managed by the Vulture Conservation Foundation (VCF) for carrying out the real tests with the birds and providing us with the data resulting from these tests.

REFERENCES

[1] A. Boulmaiz, N. Doghmane, S. Harize, N. Kouadria and D. Messadeg, "Chapter 9 - The use of WSN (wireless sensor network) in the surveillance of endangered bird species," *In Advances in ubiquitous sensing applications for healthcare, Advances in Ubiquitous Computing, Academic Press*, 2020, pp. 261-306.

[2] S. Wasserman and J. Galaskiewicz, *Advances in Social Network Analysis: Research in the Social and Behavioral Sciences*, Thounsand Oaks, CA: Sage. 1994.

[3] P. Loreti, A. Catini, M. De Luca, L. Bracciale, G. Gentile and C. Di Natale, "The Design of an Energy Harvesting Wireless Sensor Node for Tracking Pink Iguanas," *Sensors*, vol. 19, no. 5, pp. 985, 2019.

[4] P. G. Ryan, S. L. Petersen, G. Peters and D. Gremillet, "GPS tracking a marine predator: the effects of precision, resolution and sampling rate on foraging tracks of African penguins," *Mar. Biol.*, vol. 145, no. 2, pp. 215-223, 2004.

[5] M. A. Rumble, L. Benkobi, F. Lindzey and R. S. Gamo, Evaluating elk habitat interactions with GPS collars. Presented at Tracking animals with GPS: an international conference held at the Macaulay Land Use Research Institute, pp. 11-17, 2001.

[6] S. R. Jino Ramson and D. Jackuline Moni, Applications of wireless sensor networks - A survey. Presented at ICEEIMT17, pp. 325-329, 2017.

[7] D. Kandris, C. Nakas, D. Vomvas and G. Koulouras, "Applications of Wireless Sensor Networks: An Up-to-Date Survey," *Appl. Syst. Innov*, vol. 3, no. 1, pp. 14, 2020.

[8] A. Mainwaring, D. Culler, J. Polastre, R. Szewczyk and J. Anderson, Wireless sensor networks for habitat monitoring. Presented at the 1st ACM Int. Workshop Wirel. Sens. Netw. Appl., pp. 88-97, 2002.

[9] H. Wang, A. O. Fapojuwo and R. J. Davies, "A Wireless Sensor Network for Feedlot Animal Health Monitoring," *IEEE Sens. J.*, vol. 16, no. 16, pp. 6433-6446, 2016.

[10] S. Jegadeesan and G. P. Venkatesan, "Smart cow health monitoring, farm environmental monitoring and control system using wireless sensor networks", *Int. J. Adv. Eng. Technol.*, vol. VII, no. I, pp. 334-339, 2016.

[11] J. P. Domínguez-Morales, A. Rios-Navarro, M. Domínguez-Morales, R. Tapiador-Morales, D. Gutiérrez-Galán, D. Cascado-Caballero, J. Jiménez-Fernández and A. Linares-Barranco, "Wireless sensor network for wildlife tracking and behavior classification of animals in Doñana", *IEEE Commun. Lett.*, vol. 20, no. 12, pp. 2534-2537, 2016.

[12] D. García-Lesta, D. Cabello, E. Ferro, P. López and V. M. Brea, "Wireless Sensor Network With Perpetual Motes for Terrestrial Snail Activity Monitoring," *IEEE Sens. J.*, vol. 17, no. 15, pp. 5008-5015, 2017.

[13] F. Kiani, "Animal behavior management by energy-efficient wireless sensor networks," *Comput. Electron. Agric.*, vol. 151, pp. 478-484, 2018.

[14] R. Vera-Amaro, M. E. R. Ángeles and A. Luviano-Juárez, "Design and Analysis of Wireless Sensor Networks for Animal Tracking in Large Monitoring Polar Regions Using Phase-Type Distributions and Single Sensor Model," *IEEE Access*, vol. 7, pp. 45911-45929, 2019.

[15] V. Bapat, P. Kale, V. Shinde, N. Deshpande and A. Shaligram, "WSN application for crop protection to divert animal intrusions in the agricultural land", *Comput. Electron. Agric.*, vol. 133, pp. 88-96, 2017.

[16] V. Sánchez, S. Gil, J. M. Flores, F. J. Quiles, M. A. Ortiz and J. Luna, "Implementation of an Electronic System to Monitor the Thermoregulatory Capacity of Honeybee Colonies in Hives with Open-screened bottom boards," *Comput. Electron. Agric.*, vol. 119, pp. 209-216, 2015.

[17] S. Gil-Lebrero, F. J. Quiles-Latorre, M. Ortiz-López, V. Sánchez-Ruiz, V. Gámiz-López and J. J. Luna-Rodríguez, "Honey Bee Colonies Remote Monitoring System," *Sensors*, vol. 17, no. 1, pp. 55, 2017.

[18] J. Hill and D. Culler, "A Wireless Embedded Sensor Architecture for System-Level Optimization," UC Berkeley Technical Report. 2002.

[19] H. Wang, D. Estrin and L. Girod, Preprocessing in a tiered sensor network for habitat monitoring, *EURASIP J. Appl. Signal Process*, vol. 4, pp. 392-401, 2003.

[20] R. Szewczyk, E. Osterweil, J. Polastre, M. Hamilton, A. Mainwaring, D. Estrin, "Habitat monitoring with sensor networks," *Commun. ACM*, vol. 47, no. 6, pp. 34-40, 2004.

[21] V. Trifa, L. Girod, T. C. Collier, D. Blumstein and C. E. Taylor, "Automated Wildlife Monitoring Using Self-Configuring Sensor Networks Deployed in Natural Habitats," in *AROB 12th 2007*, Beppu, Japan, 2007.

[22] S. P. Pubudu Aravinda, S. Gunawardene and A. Kottege, An acoustic Wireless Sensor Network for remote monitoring of bird calls. Presented at ICIAfS16.

[23] B. Feng, B. Liu and K. Pan, "Vulture voyeur a sensor-packed egg monitors nests from the inside," *IEEE Spectrum*, vol. 53, no. 4, pp. 19-20, 2016.

[24] J. A. Gil, G. Báguena and J. M. Blanco, "Huevos con "data loggers" para el quebrantahuesos en Pirineos", *Revista Decana de la prensa ambiental Quercus: Observación, Estudio y Defensa de la Naturaleza*, vol. 364, pp. 14-15, 2016.

[25] A. Llopis and H. Frey, "La cría en cautividad del Quebrantahuesos y su problemática. En: Margalida, A. y Heredia, R. (Eds.). Biología de la Conservación del Quebrantahuesos Gypaetus barbatus en España," *Organismo Autónomo de Parques Nacionales, Madrid*, 2005, pp. 205-235.

[26] Digi International Inc. Digi XBIB-C Development Board. Xbee USB Adapter Board. Available online: `https://es.digi.com/products/embedded-systems/digi-xbee/`

digi-xbee-tools/digi-xbib-c-development-board (accessed on 7 August 2021).
[27] STMicroelectronics. NUCLEO-F303K8 - STM32 Nucleo-32 development board with STM32F303K8 MCU, supports Arduino connectivity- STMicroelectronics. Available online: http://www.st.com/en/evaluation-tools/nucleo-f303k8.html (accessed on 7 August 2021).
[28] STMicroelectronics. Mainstream Mixed signals MCUs ARM Cortex-M4 core with DSP and FPU, 64 Kbytes Flash, 72 MHz CPU, CCM, 12-bit ADC 5 MSPS, comparators, Available online: http://www.st.com/en/microcontrollers/stm32f303k8.html (accessed on 7 August 2021).
[29] Arm Limited. Arm Development Tools. Available online: https://www.keil.com/product/ (accessed on 7 August 2021).
[30] IAR Systems. IAR Embedded Workbench for Arm. Available online: https://www.iar.com/products/architectures/arm/iar-embedded-workbench-for-arm/ (accessed on 7 August 2021).
[31] Arm Limited. ARM MBED. Available online: https://os.mbed.com/ (accessed on 7 August 2021).
[32] Digi International Inc. Digi XBee SX 868 RF Module. Available online: https://www.digi.com/products/embedded-systems/digi-xbee/rf-modules/sub-1-ghz-rf-modules/digi-xbee-sx-868 (accessed on 7 August 2021).
[33] DFPlayer Datasheet. Available online: http://www.picaxe.com/docs/spe033.pdf (accessed on 7 August 2021).
[34] Kingstate Electronics Corp. KDMG12008-05 Specification for approval. Available online: http://docs-europe.electrocomponents.com/webdocs/1168/0900766b811685ce.pdf (accessed on 7 August 2021).
[35] Vishay Intertechnology Inc. Si1308EDL N-Channel 30 V (D-S) MOSFET. Available online: https://www.vishay.com/docs/63399/si1308edl.pdf (accessed on 7 August 2021).
[36] TDK InvenSense MPU-6050. MPU-6050 Six-Axis (Gyro + Accelerometer) MEMS MotionTracking™ Devices. Available online: https://www.invensense.com/products/motion-tracking/6-axis/mpu-6050/ (accessed on 7 August 2021).
[37] Sensirion. Digital Humidity Sensor SHT3x (RH/T). Available online: https://www.sensirion.com/fileadmin/user_upload/customers/sensirion/Dokumente/2_Humidity_Sensors/Datasheets/Sensirion_Humidity_Sensors_SHT3x_Datasheet_digital.pdf (accessed on 7 August 2021).
[38] Adafruit company. Adafruit Sensirion SHT31-D - Temperature & Humidity Sensor. Available online: https://www.adafruit.com/product/2857 (accessed on 7 August 2021).
[39] Shoptronica. INR21700-50E Battery Datasheet. Available online: https://www.shoptronica.com/ficheros/INR21700-50E-5000mAh-Samsung.pdf (accessed on 7 August 2021).
[40] Microchip Technology Inc. MIC5501/2/3/4. Available online: http://ww1.microchip.com/downloads/en/DeviceDoc/MIC5501-02-03-04-300mA-Single-Output-LDO-in-Small-Packages-DS20006006B.pdf (accessed on 7 August 2021).
[41] Diodes Incorporated DMP6023LE - 60V P-CHANNEL ENHANCEMENT MODE MOSFET. Available online: https://www.diodes.com/assets/Datasheets/DMP6023LE.pdf (accessed on 7 August 2021).
[42] Libelum company . LORA SX1272 Module. Available online: https://development.libelium.com/lora_networking_guide/hardware (accessed on 7 August 2021).
[43] Semtech Corporation. Semtech SX1272: Long Range, Low Power RF Transceiver 860-1000 MHz with LoRa® Technology. Available online: https://www.semtech.com/products/wireless-rf/lora-core/sx1272 (accessed on 7 August 2021).